Tuning magnetic properties with off-stoichiometry in oxide thin films: An experiment with yttrium iron garnet as a model system

Y. Dumont,[1,*] N. Keller,[1] E. Popova,[1] D. S. Schmool,[2] M. Tessier,[1] S. Bhattacharya,[3] B. Stahl,[3] R. M. C. Da Silva,[4] and M. Guyot[1]

[1]*Groupe d'Etudes de la Matière Condensée (GEMaC,) CNRS–Université de Versailles, St Quentin en Y. 45 Av. des Etats-Unis, 78035 Versailles Cedex, France*

[2]*Departamento de Fisica and IFIMUP, Universidade do Porto, Rua de Campo Alegre 687, 4169–007 Porto, Portugal*

[3]*Fachbereich Materialwissenschaft, T.U. Darmstadt, Petersenstrasse 23, D-64287 Darmstadt, Germany*

[4]*Lab. de Feixes de Iões, Dep. Física, Instituto Tecnologico e Nuclear, Sacavém, Portugal*

(Received 7 February 2007; published 13 September 2007)

We demonstrate how controlled changes in oxygen stoichiometry tune the magnetic properties and the superexchange interaction, thus providing a simple and efficient method to elaborate magnetic oxides with strongly modified magnetic and semiconductor properties. Structural and magnetic properties of the model system of yttrium iron garnet (YIG) thin films were tuned by controlling oxygen stoichiometry. The YIG phase diagram has been explored by creating cation and oxygen vacancies during film growth by pulsed laser deposition. Especially, unexplored in thermodynamic equilibrium growth conditions, excess oxygen stoichiometry in a YIG unit cell was investigated: a significant increase of Curie temperature (+10%) and magnetization (+20%) were observed. These changes are understood in the framework of a microscopic model implying the formation of Fe^{4+} and Fe^{2+} in the films with oxygen excess and vacancies, respectively.

DOI: 10.1103/PhysRevB.76.104413 PACS number(s): 75.30.Et, 61.50.Nw, 75.50.Gg, 75.70.Ak

INTRODUCTION

Control of stoichiometry is an efficient tool for tuning the physical properties of materials. This has been intensively demonstrated over the last decade in oxides with perovskite structure, where significant modifications of the electrical transport and the magnetic properties are observed with changes in the oxygen stoichiometry. Prominent examples are high T_c superconductor cuprates[1] and manganites.[2] Also, it has been recently shown that changes in oxygen stoichiometry can modify magnetic properties of simple oxides like HfO_2.[3] Another family of magnetic oxides with garnet structure has been intensively studied due to their widespread use in microwave devices. Its most prominent member is yttrium iron garnet ($Y_3Fe_5O_{12}$ or YIG). For this particular garnet an extensive body of studies has been performed on polycrystalline and single crystalline bulk material as well as for thick films grown by liquid phase epitaxy. The objectives were to fine-tune and understand the physical properties for essentially microwave and data-storage technologies with respect to the effect of substitutions and impurities (see Ref. 4). An efficient method to adjust the oxygen content and to allow considerable variations in stoichiometry is the technique of pulsed laser deposition (PLD). Growth dynamics involved in PLD is indeed in "nonthermodynamical equilibrium" as compared to bulk sample preparation.[5]

As a further step in off-stoichiometric tuning for new physical properties, we report on the model system of yttrium iron garnet. The garnet structure remains effectively robust with off stoichoimetry, either with cation substitution[6] or with oxygen treatments.[7] Since the discovery of YIG,[8] the magnetic, electrical, and structural properties of pure and substituted YIG have been intensively investigated.[6] The Ia3d cubic centered structure of stoichiometric YIG ($a = 1.2376$ nm)[6,8] consists of a closed-packed oxygen sublattice. Cations occupy all available interstitial sites: Y^{3+} on 24 dodecahedral $\{c\}$ sites, whereas Fe^{3+} both at 16 octahedral $[a]$ sites and at 24 tetrahedral (d) sites [with respective effective ionic radii 0.1019, 0.049, and 0.0645 nm (Ref. 9)]. The ferrimagnetism of stoichiometric YIG is well-described in the frame of the Néel theory:[10] the $(16a)$ and $(24d)$ Fe^{3+} sublattices are coupled antiferromagnetically, resulting in an effective moment of 5 μ_B per formula unit. Curie temperatures between 545 K (Ref. 6) and 559 K (Ref. 11) have been reported for bulk stoichiometric YIG.

EXPERIMENT

Polycrystalline YIG films were deposited onto fused silica substrates maintained at 840 °C from high purity (5N) sintered $Y_3Fe_5O_{12}$ targets. Ablation was performed with a Nd-YAG laser at 355 nm at a laser fluence stabilized slightly above the YIG ablation threshold (3 J/cm^2). One of the characteristics of the PLD growth of oxides from stoichiometric targets is the necessity to supply additional oxygen in order to restore the oxygen content of the films.[5] The total pressure in the deposition chamber was maintained at 400 mTorr by adjusting oxygen and nitrogen partial pressures. The oxygen partial pressure P_{O_2} was varied between 5 and 400 mTorr. This deposition procedure maintains similar growth conditions: same deposition rate (100 nm/h) and same rms roughness (4 nm as measured by atomic force microscopy). All film thicknesses are 200 nm. The x-ray diffraction (XRD) θ-2θ scans of the films show polycrystalline single phase of $Y_3Fe_5O_{12}$ with slight texture. Stoichiometries of the films were measured by the Rutherford back scattering (RBS) technique. Film magnetization, $4\pi M_s$, was determined by superconducting quantum interference device (SQUID) magnetometry, by ferromagnetic resonance at room temperature,

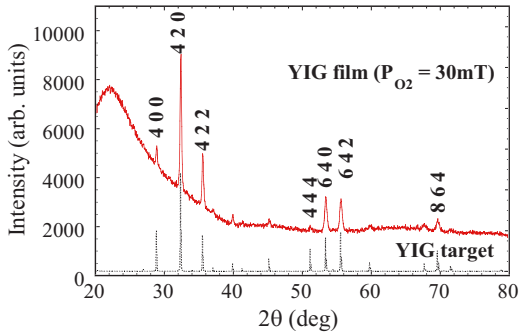

FIG. 1. (Color online) X-ray diffraction θ-2θ scan measured with the Cu-Kα wavelengths for a polycrystalline YIG film deposited on an amorphous quartz substrate at P_{stoich}=30 mTorr of oxygen pressure (red solid line) and for a polycrystalline bulk YIG reference sample (gray dotted line).

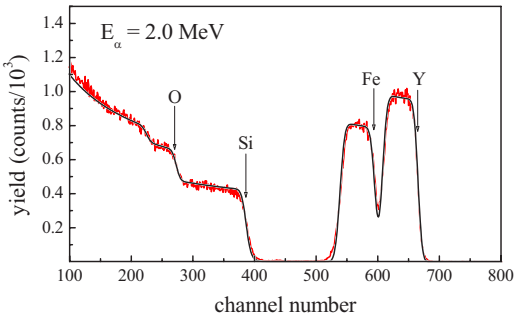

FIG. 2. (Color online) Typical RBS spectrum (online red line) determined for a polycrystalline YIG deposited at 100 mTorr of oxygen pressure and measured for a beam energy of 2.0 MeV in normal incidence.

and from magneto-optical Faraday rotation hysteresis loops. Curie temperatures T_C were deduced from the thermal variation of the specific Faraday rotation at a photon energy of 2.25 eV.

RESULTS AND DISCUSSION

In our case we find that polycrystalline YIG films grown at P_{O_2}=30 mTorr possess the crystalline structure and the magnetic properties (M_s and T_C) of the stoichiometric bulk YIG.[12] As such this pressure will be referred to as P_{stoich}. A typical θ-2θ diffraction scan is presented in Fig. 1 for a polycrystalline YIG film grown at P_{O_2}=30 mTorr. For comparison, the figure also includes the diffraction pattern taken for single phase bulk YIG. As is shown, all diffraction peaks of YIG are present in the film diffraction pattern. Closer inspection of the relative intensities of the (400), (420), and (422) diffraction peaks indicate the polycrystalline films to be slightly textured. Superimposed to the YIG diffraction peaks is the diffraction intensities of the amorphous quartz substrate with a prominent maximum at around $2\theta \sim 22°$. As will be shown below, films with P_{O_2} values different from P_{stoich} exhibit different structural and magnetic properties. RBS spectra have been measured on all YIG samples. A spectrum for a representative YIG sample is shown in Fig. 2. Several parameters can be determined from these RBS spectra. Modeling the intensity of the backscattered He atoms with a chemical concentration profile of the film allows the determination of the film stoichiometry and its thickness. Furthermore the sharpness of the retrodiffusion peaks and the absence of modification of the profile within the plateau of the peaks indicate that the films are homogeneous in composition with thickness. Further important information is contained within the shape of the rising edge of the Si-retrodiffusion peak. Its sharpness indicates that only a very limited diffusion of Si into the film is present. Modifications in cation and oxygen stoichiometry of the films, as deduced from RBS measurements, are reported in Table I for different P_{O_2}. In stoichiometric YIG, there is no possibility in its closed-packed O^{2-} structure for the interstitial sites to accommodate excesses of Y, Fe, or O without drastic lattice distortions. Consequently, films corresponding to $P_{O_2} < P_{stoich}$ have oxygen deficiencies. In particular, the film grown at 5 mTorr has 4% of oxygen vacancies (~4 vacancies per unit cell), inducing randomly localized perturbations to the oxygen lattice. Considering the global charge distribution, oxygen vacancies can act as donors[13,14] and change, in the ionic model, the iron valence to 2+ as the yttrium is stable in the 3+ state. Formation of single ionized oxygen in YIG appears less probable since the ground state of Fe^{3+} in iron oxides lies generally above the oxygen valence band,[14] thus favouring a localization of the hole near the iron ion. Therefore random Fe^{2+} are formed in the case of $P_{O_2} < P_{stoich}$. We thus conclude that for P_{O_2}=5 mTorr, resulting films have an average 8 Fe^{2+} ions among the 40 iron ions of the unit cell. On the other hand, the films corresponding to $P_{O_2} > P_{stoich}$ have iron and yttrium deficiencies. In the ionic model, since the yttrium valence is stable, this implies the formation of Fe^{4+}. From RBS results, it can be calculated that an oxygen pressure of 140 mTorr results in four iron vacancies and 2.6 yttrium vacancies per unit cell. As these act as acceptors, one has to redistribute around 20 holelike carriers per unit cell. Thus around 20 Fe^{4+} should be formed among the 40 iron sites (16 octahedral (a) and 24 tetrahedral (d)). The site occupation of Fe^{4+} in the respective a or d sites and the distribution of iron vacancies has to be considered as a function of P_{O_2}. From the charge redistribution, we can calculate the expected changes in magnetization due to the fact that both Fe^{2+} and Fe^{4+} have a lower magnetic moment ($4\mu_B$) compared to Fe^{3+} ($5\ \mu_B$).

The existence of vacancies produces localized deformations of the crystal lattice, whose overall effect can be seen

TABLE I. Atomic composition variations (ΔO, ΔFe, and ΔY) with respect to stoichiometric films deduced by RBS.

P_{O_2} (mTorr)	ΔO	ΔFe	ΔY
5	−0.04	0.00	0.00
30	0.00	0.00	0.00
140	0.00	−0.04	−0.026

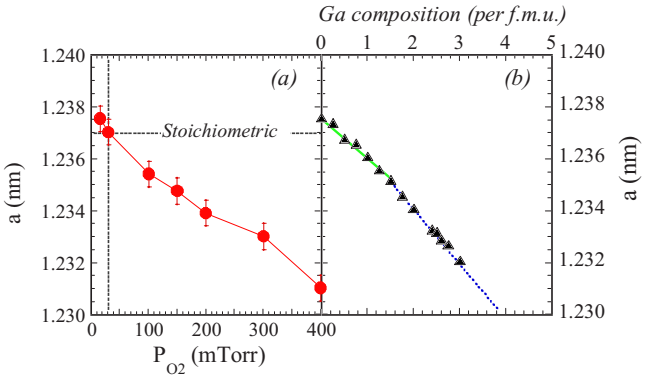

FIG. 3. (Color online) (a) YIG lattice parameter versus oxygen partial pressure P_{O_2} (plain red circles). Intersection of the dotted lines is the bulk stoichiometric film reference. (b) Lattice parameter versus x in $Y_3Fe_{5-x}Ga_xO_{12}$ (triangles) from Refs. 2 and 16. Continuous green line is the (d) site preferential substitution and dotted blue line the $(a)+(d)$ substitution.

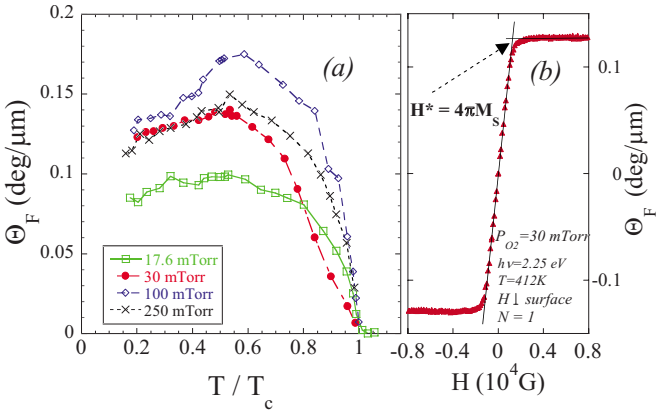

FIG. 4. (Color online) (a) Specific Faraday rotation at 2.25 eV, Θ_F, as a function of reduced temperature for samples grown with different oxygen pressures of 17.6, 30, 100, and 250 mTorr. (b) Typical magneto-optical hysteresis loop (red triangles) measured in polar configuration at 2.25 eV. H^* indicates the demagnetization field $(=4\pi M_S)$, see text for details.

as a change of lattice parameter [Fig. 3(a)]. Nevertheless, the structure determined by XRD presents, to first order, no average distortion and remains of the Ia3d space group, as the partial oxygen pressure is varied. This is verified on several inter-reticular distances (Bragg reflections 420, 422, 640, 642, and 400). The lattice parameter determined for $P_{O_2} < P_{stoich}$ presents an increase compared to its bulk value in almost the same proportions as in previous studies by Metselaar *et al.* of oxygen postannealing effects on high purity single crystals.[15] For $P_{O_2} > P_{stoich}$, the lattice parameter decreases with the increase of P_{O_2}. This region of the phase diagram was not accessible in previous studies[15] as crystal growth was performed in thermodynamic equilibrium conditions. Hence cation stoichiometry is fixed and the maximum oxygen content could not exceed 96 atoms per unit cell.

The use of PLD allows the investigation of an unexplored area of the YIG phase diagram. The effect of P_{O_2} on the lattice parameter is important and can be compared to the influence of the gallium Ga_{3+} substitution in the Fe^{3+} sites in $Y_3^{3+}Fe_{5-x}^{3+}Ga_x^{3+}O_{12}^{2-}$ with $0 \leqslant x \leqslant 5$ [Fig. 3(b)].[6,16] The substitution of trivalent nonmagnetic ions proceeds on a steric basis: those ions smaller than Fe^{3+}, such as Ga^{3+}, preferentially occupy the smaller, tetrahedral (24d) sites.[2] For increasing substitution (namely $x_{Ga} > 1.5$), Ga^{3+} ions also start to populate the larger octahedral coordinated (a) sites.[16] The steric pressure is larger for the $(16a)$ site substitution than for the $(24d)$ site as shown in the change of slope in Fig. 3(b). One can estimate the reduction of the lattice parameter per Fe^{4+} in a unit cell which is caused by the change of ion radius with the change of valence from 3+ to 4+ using the general equation $\Delta a(Fe^{3+} \rightarrow Fe^{4+}) = k_{a,d} \times (r_{Fe_{a,d}^{4+}} - r_{Fe_{a,d}^{3+}})[Fe^{4+}]$, where a and d refer to the a-site and d-site, respectively, and where r_{Fe} are the effective ionic radii ($r_{Fe_a^{4+}} = 0.0585$ nm and $r_{Fe_d^{4+}} = 0.0415$ nm).[9] The constants k have the respective values $k_a = 0.80$ and $k_d = 0.64$.[17] For 4% of Fe^{4+} per unit cell, the lattice compression are $-0.000\,35$ nm for the d-site and -0.0002 nm for the a-site compared to the measurement of -0.002 nm, which is almost ten times larger. Hence compression of the lattice parameter cannot be attributed to simple Coulomb ionic interactions only, but one has to take into account the effect of the cationic vacancies and dominant crystal field modifications.[18] These influences need more local structure determination (by extended x-ray absorption fine structure, for instance) to be precisely estimated. In any case, these localized structural distortions [changes in Fe(a)-O-Fe(d) distances and angles] will affect the superexchange mechanism between Fe(a) and Fe(b) sublattices. Their influence on the magnetization and the Curie temperature T_C are directly measured by high temperature Faraday rotation $\theta_F(H)$ hysteresis loops in polar configuration at a photon energy of 2.25 eV. Figure 4 presents the thermal variation of the specific Faraday rotation (Θ_F) measured for selected samples grown with P_{O_2} of 17.6, 30, 100, and 250 mTorr. Saturation of Θ_F was obtained at magnetic fields equal to $4\pi M_S$ (~1750 G), see Fig. 4(b). The temperature scale in Fig. 4 was normalized to the Curie temperature of each film [cf. Fig. 5(a)] in order to explicitly show the changes induced by the stoichiometry to the temperature de-

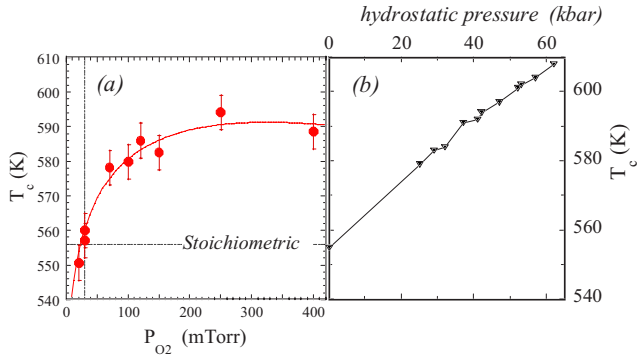

FIG. 5. (Color online) (a) Curie temperature as a function of the oxygen partial pressure P_{O_2} on YIG films (red circles). The red curve is a guide to the eye. (b) Curie temperature as a function of the hydrostatic pressure from Ref. 21 (black triangles).

pendence of the specific Faraday rotation. The variation of the Θ_F curves with temperature is characteristic for the magneto-optical response of YIG.[19] The specific Faraday rotation measured is the sum of two components, one for each of the two magnetic sublattices (i.e., the tetrahedral and the octahedral magnetic sublattice). As a result of the antiparallel alignment of the two sublattices a partial compensation occurs. Consequently, a change in the temperature dependence of Θ_F with stoichiometry indicates directly the changes in the individual sublattice magnetizations.

In Fig. 5(a), T_C is presented as a function of P_{O_2}. One observes a decrease in T_C for increasing oxygen deficiency. For $P_{O_2} > P_{stoich}$, the Curie temperature increases by up to 10% at $P_{O_2}=250$ mTorr and tends to saturate for higher oxygen pressures. A simple model can be used to describe the changes in T_C caused by the substitution of nonmagnetic metal-ion (M) to be proportional to the number, $n(y,z)$, of Fe(a)–O–Fe(d) bonds per magnetic ion, where y and z are the rate of substitution of M in a and d sites, respectively.[2] Assuming that changes in interionic distances with substitution are negligible, one can write: $T_C(y,z)=\frac{n(y,z)}{n(0,0)}T_C(0,0)$, where $n(0,0)=24/5$ represents stoichiometric YIG. This empirical model can be applied in both ($16a$) and ($24d$) site substitutions and $n(y,z)$ is always smaller in value than $n(0,0)$ for any changes in stoichiometry. Hence, generally, a decrease of T_C on substitution is to be expected. This model can be applied for the case of oxygen deficiencies ($P_{O_2} < P_{stoich}$) but is insufficient to describe the observed T_C increase for cationic deficiencies ($P_{O_2} > P_{stoich}$). In this case, the dominant effect can be related to the compression of interionic distances. From molecular field theory of a two sublattices ferrimagnet, the Curie temperature is given by the equation

$$T_C = \frac{1}{2}[(C_a N_{aa} - C_d N_{dd})^2 + 4C_a C_d N_{ad}^2]^{1/2} - \frac{1}{2}(C_a N_{aa} + C_d N_{dd}), \quad (1)$$

with $C_j=\frac{n_j(\mu_{\mathrm{eff}_j})^2}{3k_B\mu_0}$ and $N_{ij}=\frac{2z_{ij}J_{ij}}{n_i g_i g_j \mu_B^2}$, where C_j is the effective Curie constant of the jth sublattice and N_{ij} is the molecular-field constant connecting the ith and jth sublattice[10] (N_{aa} and N_{dd} are negative and $N_{ad}=N_{ad}>0$). z_{ij} represents the number of nearest neighbors on the jth sublattice that interact with the ith ion, n_i is the number of ion per mole in the ith sublattice, g_j are the respective g-factors, μ_{eff_j} are the respective effective magnetic moments, and J_{ij} is the superexchange constant. The critical coefficients in Eq. (1) are C_j and N_{ad} and their modifications with the partial oxygen pressure. J_{ad} depends on the orbital overlapping integrals and on the Pauli repulsion energy.[20] Also, as in the case of magnetic $3d^5$ transition metal (TM) ions (Fe^{3+} or Mn^{2+}), the spatial orientation of the $3d^5$ orbitals and the $2p$ oxygen orbitals result in a $3d^5$TM–oxygen–$3d^5$TM bonding angle (θ) dependence. Considering recent studies on manganite systems, in which the bandwidth has a $\cos^2(\theta)$ dependence,[21] it is possible to transpose this analytical expression in the Goodenough-Kanamori rules[7] to the Fe(a)–O–Fe(d) bond responsible for the superexchange mechanism. The following functional dependency for the superexchange integral is then determined by:

$$J_{ad} \propto \frac{b^2}{U}\cos^2(\theta) \quad (2)$$

where U is the Coulomb repulsive energy, b the exchange integral, and θ is the Fe(a)–O–Fe(d) bond angle. In the case of $P_{O_2} > P_{stoich}$, the lattice parameter decreases, therefore an increase of N_{ad} is expected as a result of the influence of the lattice parameter on b, U, and θ.

The creation of iron vacancies and the presence of related Fe^{4+} ions will decrease the effective Curie constants C_j in Eq. (1). The variation of T_C with P_{O_2} is the result of the compensation between the increasing N_{ad} factor as the lattice parameter decreases and decreasing C_j with any off-stoichiometry. For $P_{O_2} < 150$ mTorr, the N_{ad} factor is dominant. This linear variation of $T_C(P_{O_2})$ can be compared to the hydrostatic pressure (p) dependence of the Curie temperature [Fig. 5(b) and Ref. 22]. The variation ΔT_C can be linked to the lattice parameter variation Δa according to the empirical relation: $\Delta T_C=-1.25\times10^3\Delta a$.[23] For the 100 mTorr film, one calculates $\Delta T_C=37$ K due to the change of lattice parameter, which compares well with the experimentally observed shift of $\Delta T_C=28$ K [Fig. 5(a)]. As a consequence, effects of C_j are already present in the range of linear variation of T_C with P_{O_2}. So both factors are important for these oxygen partial pressures. The P_{O_2} value of 100 mTorr is significant because it corresponds to the maximum observed in magnetization at 300 K, see Fig. 6, as determined from Faraday rotation. In the case of polycrystalline YIG films, the measurement of magneto-optical hysteresis loops in polar configuration allows one to determine the magnetization directly from the magnetic external field H^* as indicated in Fig 4(b). H^* corresponds to the demagnetization field ($=4\pi M_S$) in the ab-

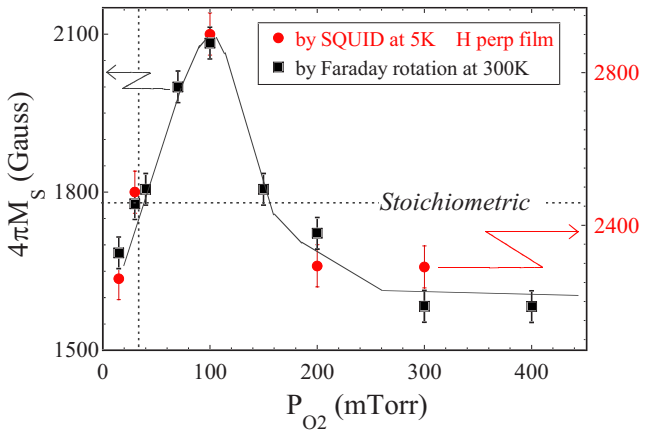

FIG. 6. (Color online) Saturation magnetization ($4\pi M_S$) at 300 K (black squares) as a function of the oxygen partial pressure P_{O_2} in YIG off-stoichiometric films, as determined by polar Faraday rotation measurements at a photon energy of 2.25 eV. Saturation magnetization (red circles) deduced by SQUID magnetometry at 5 K with H $\perp$ film plane.

sence of any significant further magnetic anisotropy field,[24] such as related to the magnetocrystalline anisotropy. As discussed elsewhere,[25] YIG is a special case as the magnetocrystalline anisotropy is an order of magnitude smaller than the dipolar fields in polar configuration. Magnetization has been measured in-plane and out-of-plane (see Fig. 6) by conventional SQUID magnetometry and determined from the angular variation of the ferromagnetic resonance (FMR) at 300 K in the X band.[26] All three techniques give similar results with a decrease in magnetization for pressures smaller than P_{stoich}, the bulk value of M_S at P_{stoich}, and a significant increase of M_s with increasing pressure ($4\pi M_S$=2100 G from FMR). For $P_{O_2} < P_{\text{stoich}}$, the decrease of $4\pi M_s$ can be related to the presence of oxygen vacancies. As a consequence the number of cations remains constant, in particular both iron sublattices remain unaltered for their occupation numbers. However, the presence of oxygen vacancies modifies globally the charge balance per unit cell. On average certain Fe ions will assume a valence state of Fe^{2+}. Hence the reduction of 4% of $4\pi M_s$ with respect to the bulk stoichiometric value can be attributed to proportional occupation of the *d* and *a* sites by the Fe^{2+} ion in the Néel approach.[18] This scenario was indeed extensively studied in the past.[2] In the opposite case of $P_{O_2} > P_{\text{stoich}}$, $4\pi M_s$ starts to increase with increasing pressure and reaches a maximum at 100 mTorr where the magnetization presents an enhanced value of $\Delta M_S/M_S$ of 20% compared to the stoichiometric value. For higher oxygen pressures, $4\pi M_s$ decreases and seems to saturate at a value of 0.1580 G for $P_{O_2} > 300$ mTorr. As mentioned earlier, for $P_{O_2} > P_{\text{stoich}}$, we have iron and yttrium vacancies and can suppose the formation of 3 Fe^{4+} ions in the vicinity of one Fe^{3+} or Y^{3+} vacancy. This situation is unexplained until now and it is more complex than simple cationic substitutions in YIG, as both iron vacancies (with no magnetic moment) and Fe^{4+} (with $4\mu_B$ moment) are simultaneously present. The difficulty is to identify on which sites (*a* or *d*) these two species are more stable. Energetic considerations need to be made.[18,27] From simple crystal electrical field considerations, the iron vacancies and the Fe^{4+} are more stable in the (16*a*) sites. The presence of Y^{3+} vacancies is equivalent to formation of three associated Fe^{4+}. In the Néel approach, the increase of $4\pi M_s$ is attributed to a reduction in magnetization of the octahedral sublattice, whereas the tetrahedral sublattice magnetization remains constant. A similar behavior was already observed for the substitution of nonmagnetic ions (Sc^{3+} and Zr^{3+}) on the (16*a*) sites.[6] A further compression of the lattice by an increasing number of Y^{3+} vacancies with higher oxygen pressure reduces the volume of both octahedral and tetrahedral sites. As a consequence, the occupation of Fe vacancies on both sublattices and their population with Fe^{4+} ions tend progressively to be more balanced, resulting in a decrease of global magnetization. More complete calculations will be presented elsewhere.[18]

CONCLUSION

We have explored parts of the YIG phase diagram, some of which are inaccessible by thermodynamic equilibrium growth conditions, using PLD as a tool to control off-stoichiometric growth by creating cation and oxygen vacancies. In particular, YIG polycrystalline thin films, grown in an oxygen atmosphere with a partial pressure superior to the stoichiometric value, exhibit metal ion deficiencies and show a significant increase in magnetization (+20%) and Curie temperature (+10%). With the "model system" of yttrium iron garnet, referenced as robust to changes in stoichiometry, we demonstrate how the magnetic properties and the superexchange interaction can be tuned by controlled changes in oxygen stoichiometry. This provides a simple and efficient method to elaborate magnetic oxides with up-to-now unexplored promising magnetic and electronic properties.

ACKNOWLEDGMENTS

The authors acknowledge very fruitful discussions with R. Krishnan and I. Maurin. This work was supported by the Ile de France Sesame Contract No. E1418 and by the bilateral GRICES(Portugal)/CNRS(France) Grant No. 14154.

*Corresponding author. yves.dumont@cnrs-bellevue.fr

[1] R. J. Cava, B. Batlogg, C. H. Chen, E. A. Reitman, S. M. Zahurak, and D. J. Werder, Nature (London) **329**, 423 (1987).
[2] K. M. Krishnan and H. L. Ju, Phys. Rev. B **60**, 14793 (1999).
[3] M. Venkatesan, C. B. Fitzgerald, and J. M. Coey, Nature (London) **430**, 630 (2004).
[4] Landolt-Börnstein, *Magnetic and Other Properties of Oxides and Related Compounds* (Springer-Verlag, Berlin, 1978), Vol. 12a.
[5] P. R. Willmott and J. R. Huber, Rev. Mod. Phys. **72**, 315 (2000).
[6] M. A. Gilleo and S. Geller, Phys. Rev. **110**, 73 (1958); M. A. Gilleo, *Ferromagnetic Materials*, edited by E. P. Wohlfarth (North-Holland, Amsterdam, 1980), Vol. 2.
[7] J. B. Goodenough, *Magnetism and the Chemical Bound* (Interscience Publishers, New York, 1963).
[8] F. Bertaut and F. Forrat, Compt. Rend. **242**, 382 (1956).
[9] R. D. Shannon and C. T. Prewitt, Acta Crystallogr., Sect. A: Cryst. Phys., Diffr., Theor. Gen. Crystallogr. **A32**, 785 (1976).
[10] L. Néel, Ann. Phys. (N.Y.) **3**, 137 (1948).
[11] E. E. Anderson, Phys. Rev. **134**, A1581 (1964).
[12] E. Popova, N. Keller, F. Gendron, L. Thomas, M.-C. Brianso, M. Guyot, Y. Dumond, and M. Tessier, J. Appl. Phys. **90**, 1422 (2001).
[13] B. Andlauer and W. Tolksdorf, J. Appl. Phys. **50**, 7986 (1979).
[14] G. B. Scott and J. L. Page, Phys. Status Solidi B **79**, 203 (1977); I. Balberg and H. L. Pinch, J. Magn. Magn. Mater. **7**, 12 (1978).
[15] R. Metselaar and M. A. H. Huyberts, J. Phys. Chem. Solids **34**, 2257 (1973).
[16] P. Fischer, W. Hälg, E. Stoll, and A. Segmüller, Acta Crystallogr. **21**, 765 (1966); A. Nakatsuka, A. Yoshiasa, and S. Takeno, Acta Crystallogr., Sect. B: Struct. Sci. **B51**, 737 (1995).
[17] B. Strocka, P. Holst, and W. Tolksdorf, Philips J. Res. **33**, 186 (1978).

[18] D. S. Schmool, Y. Dumont, N. Keller, and M. Guyot (unpublished).
[19] P. Hansen and J.-P. Krumme, Thin Solid Films **114**, 69 (1984).
[20] P. W. Anderson, Phys. Rev. **115**, 2 (1959); Solid State Phys. **14**, 99 (1963).
[21] J. L. García-Muñoz, J. Fontcuberta, M. Suaaidi, and X. Obradors, J. Phys.: Condens. Matter **8**, L787 (1996).
[22] D. Bloch, J. Phys. Chem. Solids **27**, 881 (1966); G. Bocquillon, C. Loriers-Susse, and J. Loriers, High Temp. - High Press. **5**, 161 (1973).
[23] A. K. Podsekin and V. N. Zaitsev, Sov. Phys. Solid State **23**, 160 (1981).
[24] E. Popova, N. Keller, F. Gendron, L. Thomas, M.-C. Brianso, M. Guyot, M. Tessier, and S. S. Parkin, J. Vac. Sci. Technol. A **19**, 2567 (2001).
[25] R. C. O'Handley, *Modern Magnetic Materials, Principals and Applications* (Wiley, New York, 2000).
[26] Y. Dumont, N. Keller, O. Popova, D. S. Schmool, F. Gendron, M. Tessier, and M. Guyot, J. Magn. Magn. Mater. **272–276**, 869 (2004).
[27] J. B. Goodenough, *Magnetism*, edited by G. T. Rado and H. Suhl (Academic Press, New York, 1963), Vol. III, Chap. I, p. 37.